Springer Proceedings in Physics 136

Jongmin Lee
Chang Hee Nam
Karol A. Janulewicz *Editors*

X-Ray Lasers 2010

Proceedings of the 12th International Conference on X-Ray Lasers, 30 May – 4 June 2010, Gwangju, Korea

Springer

Springer Proceedings in Physics 136

Springer Proceedings in Physics

Please view available titles in *Springer Proceedings in Physics* on series homepage http://www.springer.com/series/361/

Editors

Jongmin Lee · Chang Hee Nam
Karol A. Janulewicz

X-Ray Lasers 2010

Proceedings of the 12th International
Conference on X-Ray Lasers,
30 May–4 June 2010, Gwangju, Korea

Springer

Jongmin Lee
Advanced Photonics Research Institute
Gwangju Institute of Science and Technology
Gwangju 500-712
Republic of Korea

Chang Hee Nam
Department of Physics and
Coherent X-ray Research Centre
Korea Advanced Institute of Science
and Technology
Daejeon 305-701
Republic of Korea

Karol A. Janulewicz
Advanced Photonics Research Institute
Gwangju Institute of Science and Technology
Gwangju 500-712
Republic of Korea

Published by Springer,
P.O. Box 17, 3300 AA Dordrecht, The Netherlands
In association with
Canopus Academic Publishing Limited,
15 Nelson Parade, Bedminster, Bristol, BS3 4HY, UK

www.springer.com and www.canopusbooks.com

ISSN 0930-8989 e-ISSN 1867-4941
ISBN 978-94-007-1185-3 e-ISBN 978-94-007-1186-0
DOI 10.1007/978-94-007-1186-0
Springer Dordrecht Heidelberg London New York

Library of Congress Control Number: 2011921002

Printed on acid-free paper

Springer is part of Springer Science+Business Media (www.springer.com)

Preface

The 12th International Conference on X-Ray Lasers was held at the Gwangju Institute of Science and Technology between 30 May and 4 June 2010. The talks were presented in the International Collaboration Building belonging to the complex of the Advanced Photonics Research Institute's Ultra-short Quantum Beam Facility hosting the Korean petawatt laser system. The conference was held in Korea for the first time and gave, in a series of oral and poster sessions, a broad review of the activities in the field of coherent short-wavelength sources.

The meeting brought about 80 attendees from 14 countries in the world. It was a great pleasure for the organizers to host the many participant family members who enjoyed their first visit to such an exotic and fascinating country. The participant list confirmed a well-established core of conference visitors, but we found, not without satisfaction, that "newcomers" also enjoyed the conference and were satisfied with its environment. The event also provided an opportunity to publicize X-ray laser research to the Korean based science community and to boost X-ray laser research in Korea.

The conference program was organized to promote closer contacts and better understanding between different subfields of the research into coherent short-wavelength radiation sources. That was the reason for organizing separate sessions dedicated to X-ray Free Electron Lasers (XFELs), sources based on relativistic interaction with matter and incoherent sources in both the keV and XUV spectral ranges. This aspect is not fully covered by this book for different reasons, but it was interesting to observe that the idea "caught on". The conference confirmed the well-established status of X-ray lasers with their well-understood physics, and presented intriguing questions to be answered for further progress and development. This point was clearly supported by the increased number of contributions relating to applications of the short-wavelength sources.

The scientific schedule of the conference was supplemented by a social program, including trip to an amazing ecological system of the Suncheon Bay, a wetland preservation area registered in the Ramsar convention. The conference dinner, held in the Oryong Hall – the GIST convention center – was preceded by a stunning demonstration of traditional Korean music and dance. This event culminated in a joint performance by the artists and conference attendees.

There were many people who contributed to the successful organization of the conference. We are not able to list all of them but we would like to express our special gratitude to Drs Chul Min Kim, Hyung Taek Kim and I Jong Kim as well as to Mrs Ga Young Cha and Mr Ho Jong Kang from APRI staff. In addition, we acknowledge the generous sponsorship from the Gwangju Convention and Visitors Bureau, Korean Physical Society, Optical Society of Korea, the Ultra-Short Quantum Beam Facility Program of the Ministry of Knowledge Economy of Korea, Korea Electro-Optics, DPI, Dada, Laser Spectra, CVI Melles Griot, Coherent, Horiba Korea Ltd., Jinsung Laser, Alcatel Korea, Golden Light Co., Lee Optics, Qbic Laser System Inc. and Thales Laser.

Finally, we owe a pleasant debt of appreciation to the conference attendees and contributors for their willingness to participate in the conference and finally to contribute to this book.

Jongmin Lee
Chang Hee Nam
Karol A. Janulewicz


12th International Conference on X-Ray Lasers
May 30 – June 4, 2010 Ultrashort Quantum Beam Facility
Hosted by APRI GIST
Sponsored by
apri
고등광기술연구소

Contents

Part 1: X-Ray Laser Systems 1

Recent results and future plans for XRLs using the TARANIS laser facility 3
C.L.S. Lewis, T. Dzelzainis, D. Riley, D. Doria, S. White, M. Borghesi, G. Narsisyan, D. Marlow, K. McKeever and G.J. Tallents

Source development and novel applications of laser-driven plasma X-ray lasers in JAEA 15
T. Kawachi, N. Hasegawa, M. Nishikino, M. Ishino, T. Imazono, T. Ohba, T. Kaihori, M. Kishimoto, Y. Ochi, M. Tanaka, M. Koike, M. Kado, K. Namikawa, T. Suemoto, K. Terakawa, T. Tomita, M. Yamamoto, N. Sarukura, H. Nishimura, A. Y. Faenov, S. Bulanov, H. Daido and Y. Kato

Theoretical study of Ni-like Ta XRL driven by one 2ω pulse with duration of 100 ps on upgraded ShenguangII facility 25
Z. Guoping, Q. Xiumei, Z. Wudi

X-ray laser developments at PHELIX 31
B. Zielbauer, T. Kuehl, B. Aurand, V. Bagnoud, B. Ecker, U. Eisenbarth, D. Hochhaus, P. Neumayer, D. Zimmer, K. Cassou, S. Daboussi,, O. Guilbaud, J. Habib, S. Kazamias, D. Ros, J. Seres, C. Spielmann

LASERIX : an open facility for developments of EUV and soft X-ray lasers and applications 39
D. Ros, K. Cassou, B. Cros, S. Daboussi, J. Demailly, O. Guilbaud, G. Jamelot, J. Habib, S. Kazamias, J.-C. Lagron, G. Maynard, O. Neveu, M. Pittman, B. Zielbauer, D. Zimmer, T. Kuehl, V. Bagnoud, F. Delmotte, D. Joyeux, S. De Rossi, A. Klisnick, S. Lacombe, C. Le Sech, E. Porcel, M.-A. du Penhoat, A. Touati, P. Zeitoun, J.-P. Chambaret, F. Mathieu and G. Mourou

Using the X-FEL as a source to investigate photo-pumped X-ray lasers 47
J. Nilsen and H. A. Scott

Part 2: Repetitive X-Ray Lasers 55

Demonstration of an all-diode-pumped soft X-ray laser and other advances in table-top soft X-ray lasers 57
J. J. Rocca, B. Reagan , F. Furch, Y. Wang, D. Alessi , D. H. Martz , M. Berrill, V.N. Shlyaptsev, B. M. Luther, A. H. Curtis

Saturated XUV lasing down to 8.85 nm using the grazing-incidence scheme 69
J.E. Balmer, C. Imesch, and F. Staub

Double-pulse single-beam grazing-incidence pumping (DGRIP) 77
D. Zimmer, B. Zielbauer, M. Pittman, O. Guilbaud, J. Habib, S. Kazamias, D. Ros, V. Bagnoud, and T. Kuehl

Development and application of plasma-waveguide based soft X-ray lasers 83
Jiunn-Yuan. Lin, Ming-Chang Chou, Ping-Hsun Lin, Ru-Ping Huang, Szu-Yuan Chen, Hsu-Hsin Chu and Jyhpyng Wang

Development of silver tape target system for high repetition X-ray laser 93
Masaharu Nishikino, Yoshihiro Ochi, Noboru Hasegawa, Tetsuya Kawachi, Toshiyuki Ohba, Takeshi Kaihori, and Keisuke Nagashima

Part 3: X-Ray Laser Amplifiers – Seeding 99

Temporal coherence and spectral width of seeded and ASE XUV lasers 101
A. Klisnick, O. Guilbaud, ,J.P. Goddet, F. Tissandier, L.M. Meng, , L. Urbanski, J. Gautier, S. de Rossi, D. Alessi ,Y. Wang, B. Luther, D. Martz, S. Domingue,, G. Maynard, D. Benredjem, A. Calisti, S. Sebban, M. Marconi , D. Joyeux , J.J.Rocca

Wave perspective on high harmonics amplification in a high-gain medium with level degeneracy 111
C. M. Kim, K. A. Janulewicz, and J. Lee

Laser driven parametric amplification in the xuv and soft-X-ray spectral range 121
J. Seres, E. Seres, D. Hochhaus, B. Ecker, D. Zimmer, V. Bagnoud, T. Kuehl, C. Spielmann

Characterization of a seeded optical-field ionized collisional soft X-ray laser 127
S. Sebban, F. Tissandier, J.P. Goddet, O. Guilbaud, J. Gautier, Ph. Zeitoun, C. Valentin, G. Lambert, G Maynard, B.Robillard, A. Klisnick, T. Mocek and J. Nejdl

Optimization of soft X-ray amplifiers by tailoring plasma hydrodynamics 137
E. Oliva, Ph. Zeitoun, P. Velarde, M. Fajardo, K. Cassou, D. Ros, D. Portillo and S. Sebban

Measurement of the temporal coherence of a seeded GRIP transient Mo soft X-ray laser 143
L.M. Meng, D. Alessi, O. Guilbaud, Y. Wang, S. Domingue, B. Luther, J.J. Rocca and A. Klisnick

Part 4: Sources Based on Relativistic Interaction 149

Extreme field limits in the ultra-relativistic interaction of electromagnetic waves with plasmas 151
S. V. Bulanov, T. Zh. Esirkepov, M. Kando, J. K. Koga, A. S. Pirozhkov, Y. Kato, S. S. Bulanov, G. Korn, and A. G. Zhidkov

Generation of coherent X-ray radiation with relativistic nonlinear processes 183
Y. Kato, M. Kando, A. S. Pirozhkov, T. Zh. Esirkepov, K. Kawase, H. Daido, H. Kiriyama and S. V. Bulanov

Part 5: High-harmonics 195

Generation of ultrashort attosecond high-harmonic pulses from chirp-compensated Ne harmonics 197
Dong Hyuk Ko, Kyung Taec Kim, Juyun Park, Jae-hwan Lee and Chang Hee Nam

An intense kHz and aberration-free two-color high harmonic source for seeding FEL and XRL 203
G. Lambert, J. Gautier, C.P. Hauri, F. Tissandier, C. Valentin, A. Barszczak Sardinha, M. Fajardo, T. Marchenko, J.Ph. Goddet, M. Ribiere, G. Rey, S. Sebban and Ph. Zeitoun

Tuning of high-order harmonics for soft X-ray laser seeding 209
Boris Ecker, Bastian Aurand, Daniel C. Hochhaus, Thomas Kuehl, Bernhard Zielbauer, Daniel Zimmer, J. Seres, C. Spielmann

Generation of small band width coherent extreme ultraviolet radiation and its application 215
L.V. Dao, S. Teichmann, K.B. Dinh, and P. Hannaford

Highly directive high harmonic generation from solid target plasma for biomedical and medicine applications 221
H. Kuroda, M. Baba, R. A. Ganeev, M. Suzuki, S. Yoneya

High harmonic generation by using laser-ablation two-compounds target scheme 231
M. Suzuki, M. Baba, R. A. Ganeev, and H. Kuroda

Part 6: Incoherent Short-Wavelength Sources 237

EUV-induced surface modification of polymers 239
A. Bartnik, H. Fiedorowicz, R. Jarocki, J. Kostecki, M. Szczurek , A. Biliński, O. Chernyayeva, J.W. Sobczak

Study on fundamental processes of laser welded metals observed with intense X-ray beams 245
T. Muramatsu, H. Daido, T. Shobu, K. Takase, K. Tsukimori, M. Kureta, M. Segawa, A. Nishimura, Y. Suzuki and T. Kawachi

XUV radiation emitted by capillary pinching discharge 257
M. Vrbova, A. Jancarek, P. Vrba, M. Nevrkla and P. Kolar

EUV radiation of pulse high-current proximity-wall-stabilized discharges 263
K. Kolacek, J. Straus, J. Schmidt, O. Frolov, V. Prukner, , J. Sobota, T. Fort and A. Shukurov

Part 7: X-Ray Laser Applications 269

Probing high energy density plasmas with EUV and X-ray lasers 271
G J Tallents, L M R Gartside, A K Rossall, E Wagenaars, D S Whittaker, M Kozlova, J Nejdl, M Sawicka, J Polan, M Kalal and B Rus

Measuring the electron density gradients of dense plasmas by X-ray laser deflectometry 281
J. Nejdl, M. Kozlová, T. Mocek, B. Rus

Laser-matter interaction studies using X-ray laser and double Lloyd's mirror interferometer 293
M. Kozlova, J. Nejdl, B. Rus, M. Sawicka, J. Polan, L. Gartside, A. Rossall, G. Tallents

Application of laser plasma x-ray beam in radiation biology 301
Masaharu Nishikino, Katsutoshi Sato, Noboru Hasegawa, Masahiko Ishino, Tetsuya Kawachi, Takashi Imazono, Hodaka Numasaki, Teruki Teshima, and Hiroaki Nishimura

Energy spectra of photo- and Auger electrons generated by a soft X-ray laser and Xe cluster interaction 307
S. Namba and N. Hasegawa, M. Kishimoto, M. Nishikino and T. Kawachi

Observation of phase transition dynamics in BaTiO3 by X-ray laser speckle technique 313
K. Namikawa, M. Kishimoto, R. Z. Tai, K. Nasu, E. Matsuhita

Single-shot nanometer-scale Fourier transform hologram using Ni-like Ag X-ray Laser 323
H. T. Kim, I J. Kim, C. M. Kim, T. J. Yu, S. K. Lee, J. H. Sung, J. W. Yoon, H. Yun, T. M. Jeong, I. W. Choi, and J. Lee

Theory and computations towards coherent reflection imaging of tilted objects 329
I. A. Artyukov, A.N. Mitrofanov, A.V. Popov, N.L. Popov and A.V. Vinogradov

Highly efficient soft X-ray microscope using PMMA phase-reversal zone plate 341
Kyoung Hwan Lee, Seung Beom Park, Jong Ju Park, Deuk Su Kim, Ju Yun Park, Jae-hwan Lee and Chang Hee Nam

Single-photon ionization soft-X-ray laser mass spectrometry of potential hydrogen storage materials 347
F. Dong , E.R. Bernstein and J.J. Rocca

Development of the X-ray interferometer and the method of spatial and temporal synchronization of XRL and optical pulse 353
N. Hasegawa, Y. Ochi, T. Kawachi, K. Terakawa, T. Tomita, M. Yamamoto, M. Nishikino, T. Ohba, T. Kaihori, T. Imazono, A. Sasaki, M. Kishimoto, M. Ishino, M. Kado, M. Tanaka, T. Nakazato, N. Sarukura and T. Suemoto

Reflection microscope for actinic mask inspection and other progress in soft x-ray laser nano-imaging 359
C. S. Menoni, F. Brizuela, S. Carbajo, Y. Wang, D. Alessi, D. H. Martz, B. Luther, M. C. Marconi, J. J. Rocca, A. Sakdinawat, W. Chao, Y. W. Liu, E. H. Anderson, K. A. Goldberg, D. T. Attwood, A. V. Vinogradov, I. A. Artioukov, B. LaFontaine

Part 1: X-Ray Laser Systems

Recent results and future plans for XRLs using the TARANIS laser facility

C.L.S. Lewis[1], T. Dzelzainis[1], D. Riley[1], D. Doria[1], S. Whyte[1], M. Borghesi[1] G. Nersisyan[1], D. Marlow[1], K. McKeever[1] and G.J. Tallents[2]

[1] Center for Plasma Physics, Queen's University Belfast, Belfast, BT9 5ED
[2] Physics Department, University of York, Y010 5DD, UK.

Abstract. The results of an investigation into X-ray lasing in Ni-like Sm, pumped by a frequency doubled pre-pulse and a fundamental short pulse, are presented. Strong lasing was observed across the $4d_{3/2}$-$4p_{3/2}$ transition at 7.3 nm. A weaker laser line of wavelength 6.9 nm was also present from the $4d_{3/2}$-$4p_{1/2}$ transition. The XRL output was seen to be sensitive to both delay between the pre-pulse and the heating pulse and also to the energy in the heating pulse. The results are compared to those from a similar experiment employing pre-pulses at the fundamental wavelength and the output of the XRL is shown to be enhanced by at least two orders of magnitude for the same target lengths. An application for an XRL pumped by Taranis is discussed.

1 Introduction

Lasing in the region below 10 nm using a ~psec pump pulse been has been the subject of a limited number of experimental investigations [1],[2]. Extending the scheme to elements heavier than Sm poses problems. Firstly, the psec scheme employs a time delay between the pre-pulse and the main pulse to allow the plasma to expand. This reduces density gradients and subsequently refraction of the XRL pulse in the plasma to a point where the pulse can propagate the entire length of the plasma within the gain region. This must be balanced against the cooling of the plasma with expansion, so that a peak delay is found where the density gradients are sufficiently shallow, but the plasma is still at the required ionisation stage. With higher Z-elements, the higher temperature required to achieve a substantial Ni-like population, and the increased electron density required to increase the collisional excitation rate to compensate for the increased radiative decay rate between the laser levels requires the delay to be shorter until the point is reached where the optimum time for the pump pulse is almost directly after the pre-pulse, into steep density gradients. This is usually the case for elements with Z>62 (Sm). For higher Z-number elements the additional problem arises of the optimum pumping density being higher than the critical density of Ti:Sapphire and Nd:Glass systems, which are commonly used XRL pump lasers. The problem

J. Lee et al. (eds.), *X-Ray Lasers 2010,* Springer Proceedings in Physics 136,
DOI 10.1007/978-94-007-1186-0_1, © Canopus Academic Publishing Limited 2011

of the high density gradients can be overcome by using a combination of second harmonic pre-pulse and fundamental main pulse. This allows the plasma/solid interface to be pushed back to higher densities than the region pumped by the main pulse, allowing the high temperatures, high densities and shallow density gradients to co-exist. The dynamics of short wavelength x-ray lasers pumped with ~ps pulses was the subject of a recent study by Pert [3],[4] where simulations of XRLs pumped with a laser such as VULCAN, using the second harmonic for the prepulse and the fundamental wavelength for the main heating pulse are discussed. The studies by Pert form the theoretical basis for the following experiment. Two colour pumping has previously been investigated with lower Z-number targets and was found to enhance the output of a Ni-like Ag XRL at 13.9nm and, furthermore, stimulate emission on a previously unobserved line identified as the $4f\,^1P_1 - 4d\,^1P_1$ transition [5].

2 Experimental Configuration

The experiment was carried out at the Central Laser Facility, UK and the chamber layout is shown in Figure 1.

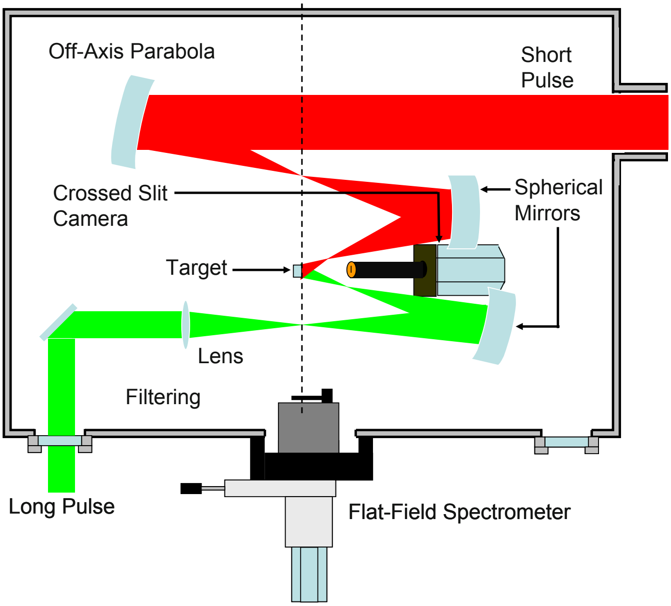

Fig 1. Experimental layout for investigation into short wavelength lasing with two-colour pumping.

The pre-plasma is formed by one or two ~300 ps, frequency-doubled beams, focussed to a line of nominal length 6 mm by identical focusing systems. The focusing system consists of a lens followed by a tilted spherical mirror, giving a near normal incidence line focus. The beams were able to focus at the same point in the chamber by exploiting the cylindrical symmetry of the optical system about the XRL axis. Energies up to 120 J were available in second harmonic for the pre-pulse, giving a maximum possible average irradiance of 3×10^{14} Wcm^{-2} on target. The short pulse was focussed initially by an off-axis-parabola, and then allowed to expand before being focussed to a line by the tilted spherical mirror. Energies up to 100 J in a pulse of ~750 fs were available at the fundamental wavelength, giving a maximum possible average irradiance of ~10^{17} Wcm^{-2}. Traveling wave pumping was achieved by the tilting of the wave-front by insertion of a grating into the beam path before it entered the target area. This is a technique that has been employed successfully on Vulcan in previous experiments [6][7]. The traveling wave speed was measured with an optical streak camera to be ~0.94c. Samarium coated glass slabs were placed at the overlap position of the three beams. A crossed slit camera was used to observe the uniformity and overlap of the line foci. This observed the plasma column from below the experimental plane. A crystal spectrometer with a KAP crystal, positioned above the experimental plane confirmed the presence of Ni-like ions in the plasma as in Figure 2.

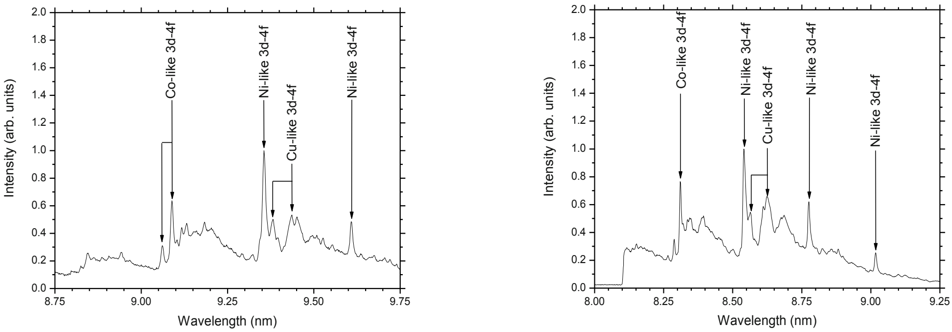

(a) (b)

Fig 2. Spectral line-outs from the crystal spectrometer showing Ni-, Co- and Cu-like emission. Although the line ratios are similar in Sm (a) to those observed in Gd (b) only the Sm targets showed strong laser action.

3 Results

3.1 Samarium

Strong lasing was observed for Samarium targets with 40-50 J in the pre-pulse (average irradiance ~10^{14} Wcm^{-2}) and 60-70 J in the short pulse (average irradiance ~5×10^{16} Wcm^{-2}). A spectral line-out of a strong laser shot using these energies is shown in Figure 3. Two lasing lines are seen in first and second order. The strongest emission was observed at 7.3 nm arising from the

$4d_{3/2}$-$4p_{3/2}$; lasing is also seen on the $4d_{3/2}$-$4p_{1/2}$ transition, but considerably weaker. Figure 4 shows the angular distribution of the two laser lines. The stronger line is fitted with a Gaussian centred at 5.32 ± 0.03 mrads and with a FWHM of 5.56 ± 0.09 mrads.

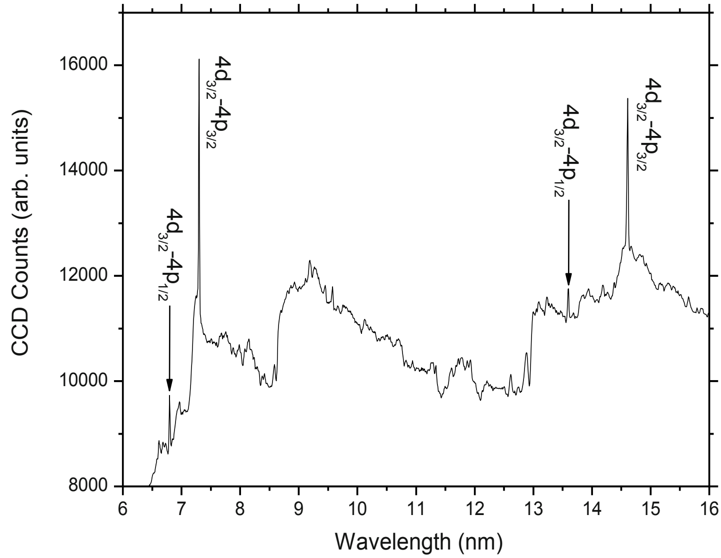

Fig 3. Spectral line-out of the image obtained from the FFS. The two Sm XRL lines are seen in first and second orders. The $4d_{3/2}$-$4p_{3/2}$ is seen to dominate the spectrum.

The output of the XRL was observed to vary with both the energy in the CPA beam and delay between long and short pulses. Figure 5 (LHS) gives a summary of the measured XRL output at varying delay and with differing energy in the CPA and long pulses. The data taken with 30-40 J in the CPA and 40-50 J in the long pulse suggests maximum output at delays between 100 and 150 ps, with low signal seen at 50 ps and no lasing observed at 200 ps. The shots taken with 60-70 J in the CPA pulse and 40-50 J in the long pulse with a 150 ps delay show a much higher energy output than for the 30-40 J data. There is also slightly increased emission at 200 ps when 110-120 J were used in the long pulse and 60-70 J in the CPA. Time constraints prevented a full parameter scan being carried out and so the information about the behaviour of the XRL output with respect to pump energy and delays is very limited. The dependence on short pulse energy of the XRL output suggests that the short pulse energy was near the threshold for generation of laser action.

In order to assess the success of this pumping scheme, we can compare the results to those reported by King et al [2]. Such a comparison requires confidence in the data analysis procedures used in each case (ie different experiments and different detector setup). We have used a rigorous approach to make reliable estimates of all the relevant factors (eg counts to energy conversion, QE of CCD, filter transmissions, grating efficiency etc) and in all cases where there is uncertainty we have erred on the side of reducing the "measured" XRL energy. In reference [2] the fundamental wavelength was

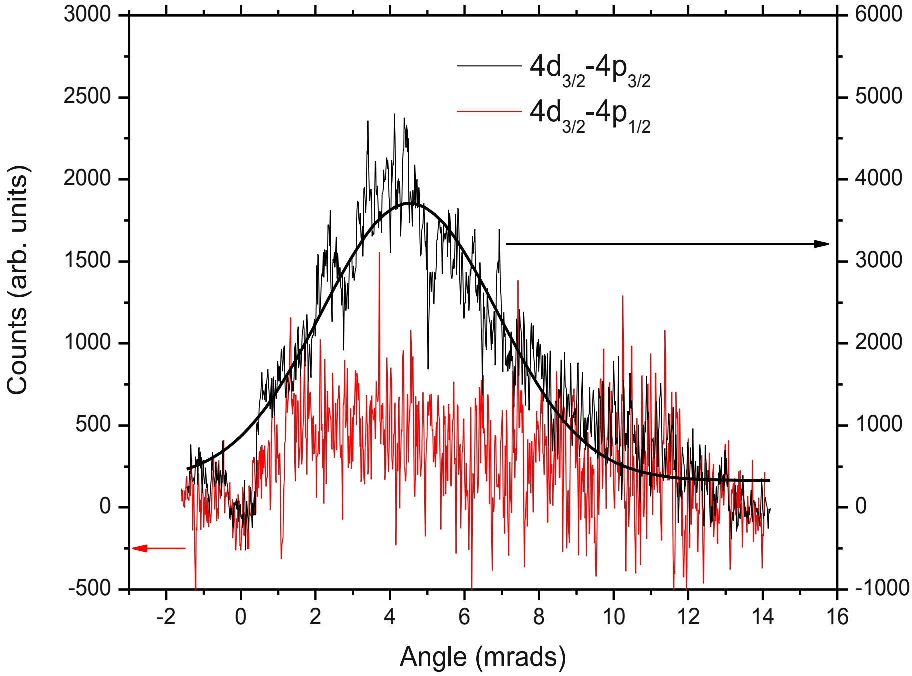

Fig 4. Angular distributions of the two lasing lines. The stronger $4d_{3/2}$-$4p_{3/2}$ line is fitted with a Gaussian curve centred at 5.32 ± 0.03 mrads, with a FWHM of 5.6 ± 0.1 mrads

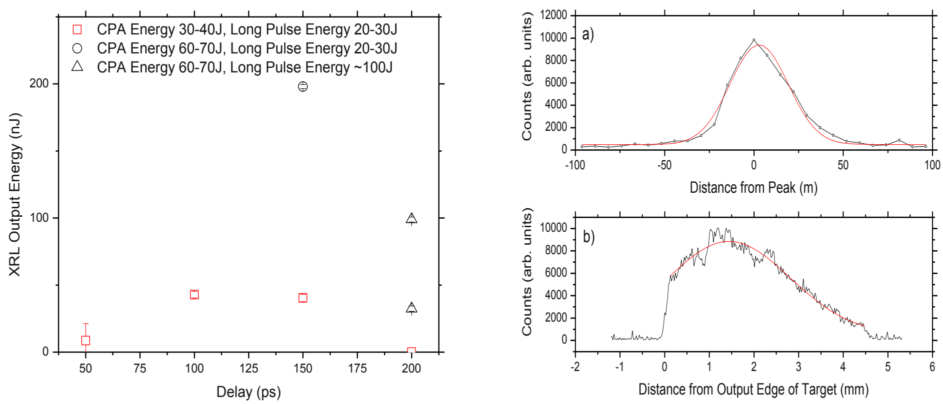

Fig 5. (LHS) Summary of the Sm XRL energy for a range of pumping conditions with 5 mm long targets and (RHS) Line focus profiles in the directions perpendicular a) and parallel b) to the XRL axis.

used for the pre-pulse with an irradiance of ~1 × 10^{13} Wcm^{-2} and pulse duration 280 ps, which is similar to the irradiance and pulse duration used in this experiment to obtain strong lasing in Sm (2×$10^{13}$$Wcm^{-2}$). In reference [2], the pump pulse used had an intensity of ~3 × 10^{15} Wcm^{-2} with a duration of 3 ps, and the XRL energy output was ~1nJ for target lengths of 5 mm. As shown in Figure 5 (LHS), the two colour pumping method demonstrated here produced an XRL output of ~50 nJ for 5 mm target lengths using an energy of 30-40J in the pump pulse and ~200nJ of XRL energy using an energy of 60-70J in the pump pulse, corresponding to pump pulse intensities of ~1.5-2.9 × 10^{16} Wcm^{-2}. Some of the observed fluctuation in output can be attributed to line focus alignment issues. Profiles of the linefocus used in this experiment are shown in Figure 5 (RHS). The transverse profile is fitted with a Gaussian with a FWHM of 38 ± 6 μm. The axial lineout is fitted with a Gaussian with a FWHM of 3.2 ± 0.1 mm. The intensity profile shows strong emission at the output end of the XRL target, but due to the short linefocus length slightly underfills the 5 mm target. The linefocus width was seen to vary from shot to shot, reaching up to 100 μm FWHM. The asymmetry in the wider line foci suggest this was due to misalignment between the long and short pulses. It is likely that this added to the lack of reproducibility of the XRL which was also affected by fluctuations in the energy output of the VULCAN laser itself.

Although the data is limited we are nevertheless confident that that the range of outputs observed (circa 100 nJ) with 2ω-ω pumping is about 100 times higher than observed previously (circa 1 nJ) with ω-ω pumping. Also, it has to be appreciated that the pump pulse used in the current experiment was measured to be more than 4 times shorter than that used by King et al, meaning that the energy densities along the 5 mm line focus conditions in the two experiments are, in fact, very similar.

Modeling of the previous experiment was presented in [3] where it was concluded that the highest gain generated was in a region of steep density gradients which prevented efficient amplification in this region but that a region of reduced gain present further from the target in a region of lower density gradients was sufficient to observe significant output. The large increase in output energy observed supports the predictions made by the simulations that the second harmonic pre-pulse is generating a plasma with reduced density gradients at the turning point for the short pulse, and hence allowing effective XRL pulse propagation in the high electron density, and hence high gain, region.

3.2 Gadolinium and Dysprosium

Unsuccessful attempts were made to use this method to produce XRL output from Ni-like Gd and Ni-like Dy. Spectra obtained from the crystal spectrometer show that the plasma reached the Ni-like ionisation stage but failed to show lasing action. The spectrum from Gd (see Figure 2b) showed line ratios extremely similar to those seen for a Sm target which produced strong lasing. Attempts to observe lasing were made with energies in the long pulse far in excess of those suggested necessary by simulation to achieve the correct ionisation stage in the pre-plasma, implying that the Ni-like population shown to be present by the crystal spectrometer data was generated during the long pulse, and not the result of a pre-plasma with lower than required ionisation being further heated by the main pulse. Unfortunately no spectra were obtained for shots using the long pulse only. We would also not have expected that high energy in the long pulse would have heated the plasma to the point where it is over-ionised, since lasing was observed in Sm for the highest long pulse energies. The problem is likely to lie with the main pulse and a failure to sufficiently raise the electron temperature to the point where effective gain generation occurs. The short pulse was measured during this experiment to be ~700 fs (ie shorter than the ~ 2 psec expected) and probably not optimum for efficient heating of the electrons.

4 XRL data from TARANIS

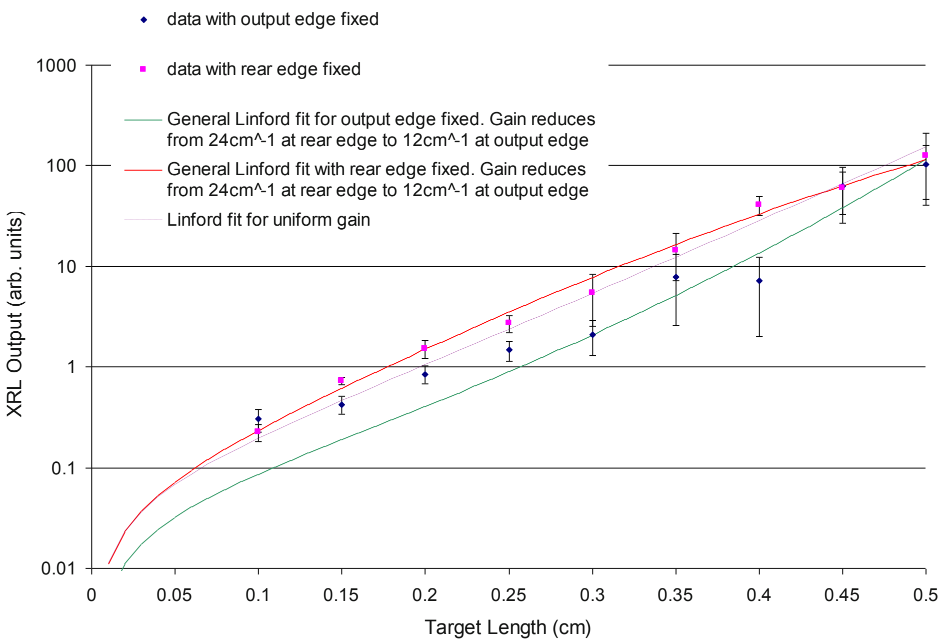

Fig 6. Growth curves for the $4d_{3/2}$-$4p_{3/2}$ line of Ni-like Mo at 18.9 nm showing asymmetry based on choice of where to fix the target edge within the line focus.

We have reported previously on preliminary saturated XRL output from Ni-like Mo and Ag targets pumped in the GRIP mode by the dual beam CPA laser housed in QUB [8],[9],[10]. During these investigations issues were raised as to the interpretation of growth curve shapes. To help elucidate the various factors, Figure 6 depicts an example where we have used right-angled triangular targets of sheet Mo mounted so that the vertical edge can be kept in a fixed location relative to the line focus pump distribution as the target is raised/lowered to access new lengths for shooting. The maximum target length (5 mm) was centred to align with the line focus but in one sequence the fixed edge was closest to the observing FFS (XUV flat field spectrometer) and in the second sequence it was furthest away. Several shots were taken for all lengths shot to monitor reproducibility and Figure 6 shows that a real trend exists. At the shortest and maximum lengths in each case XRL output is similar but the growth curves have clearly different shapes. In this particular case, it is probably mainly due to non-uniformity of pump intensity along the line affecting the local gain coefficient but amplification details can also be affected by axial variation of the travelling wave velocity and the spatial location (in the normal direction to the target surface) of the peak gain zone. Both of these are dependent on the optics focussing the heating pulse in the GRIP scenario and their optimisation will be a topic for future reports.

Analytical and numerical modelling can help design optimum conditions and experimentally these can be tested. Velocity mis-matches can be tested through "tilting" wave fronts and/or varying short pump pulse durations; axial pump uniformity can be controlled with phase plates and/or shaped masks in pump beam; the spatial gain zone envelope within the plasma can be controlled with F-number/optics to minimise XRL refractive "walk off", all of these need to be compatible with the most efficient pump coupling possible.

5 WDM probed by an XRL beam

The acceleration of proton beams from laser-irradiated solid targets has been investigated employing the TARANIS laser system operating in the compressed pulse mode. The laser pulse from one of the main compressors was focused onto a thin metal foil with an f/3, f = 300 mm off-axis parabola (OAP). The pulse after compression was ~ 10 J in energy and ~ 560 fs in duration, and the focal spot diameter (measured in the low power, non amplified mode) was ~ 10 μm, leading to an intensity on target ~ 5 × 10^{18} Wcm^{-2}. The targets were Aluminium foils of thickness ranging from 0.7 to 100 μm. The proton beam emitted from the rear target surface (i.e. the non-irradiated surface) in the target normal direction was detected employing multi-layer stacks of Gafchromic type HD-810 Radiochromic Films (RCFs). The RCF packs were wrapped in 11 μm aluminium foils in order to cut unwanted heavy ion and soft x-ray signals and to shield the pack from target debris, therefore giving a minimum detectable proton energy of about 1 MeV. The multi-layer arrangement of the RCF stacks ensured a spectral multi-frame capability of the detection system. Protons with higher energies penetrate deeper in the stack and release their energy mainly in proximity of the Bragg peak. Each film in the stack acts as a filter for the following ones and spectrally selects the protons whose Bragg peak is localized within or in proximity of the active layer. Data from a typical RCF stack shows a spectrum resembling a truncated Boltzmann-like distribution, with a temperature of 2.3 ± 0.1 MeV, with small variations depending on the target thickness and with small shot to shot fluctuations. The total number of particles accelerated in a single shot is ~ 5×10^{11}, corresponding to a integrated particle energy of ~ 0.5 J for particles with energy above 3 MeV (~ 1 J considering particles above 1 MeV) and to an efficiency in the conversion from laser energy into energetic protons of 0.5% (~ 1%). The dependence of the maximum proton energy on the target thickness was also investigated and a maximum proton energy of ~ 12 MeV was obtained for a target thickness between 6 and 10 µm. A detectable proton beam was accelerated for targets as thin as 1 µm, which is an indication of the high contrast level of the TARANIS laser system.

Since we have the capability of combining proton beams and XRL beams it is of interest to consider how they can be usefully applied. A possible scenario

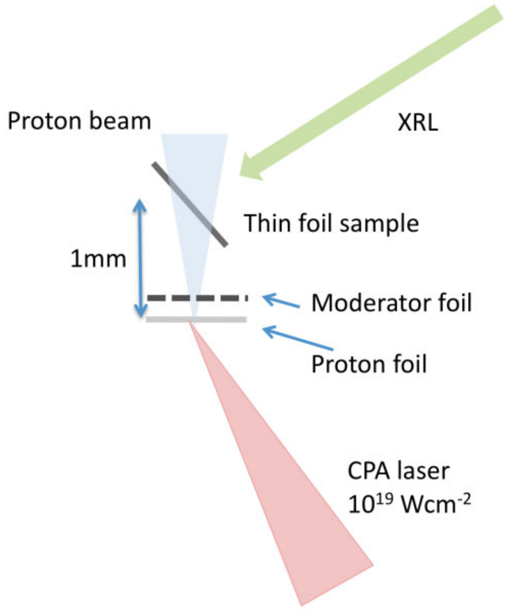

Fig 7. Schematic of a possible opacity experiment on proton heated matter. It is feasible for TARANIS to synchronously generate both the proton and XRL pulses.

is illustrated in Figure 7 whereby protons heat a thin foil to a few eV at near solid density and an XRL is used to makes opacity measurements of the resultant WDM.

Because there is a range in proton energies and a finite distance to the sample foil, the energy is deposited over a finite time as depicted in Figure 8a where we can see the temporal history of the deposition in a thin slice of the foil, buried 10 microns into the foil. This is simulated by assuming all energy is deposited into electrons and inserting this profile as an electron heating term into the Hyades hydrodynamic code for a case where we have a 10 micron thick moderator foil that slows the protons before they enter an 0.8 micron Al foil where they deposit energy uniformly in space but with the temporal history of Figure 8a. The resultant profile of density and temperature at the end of the heating pulse of protons is depicted in Figure 8b, where the density has remained high and the temperature has reached ~1.5eV. This will provide a benchmarking parameter for detailed hydrodynamic simulations comparing the effects of changing the equation of state and/or ionisation model on the hydrodynamic conditions and predicted opacity.

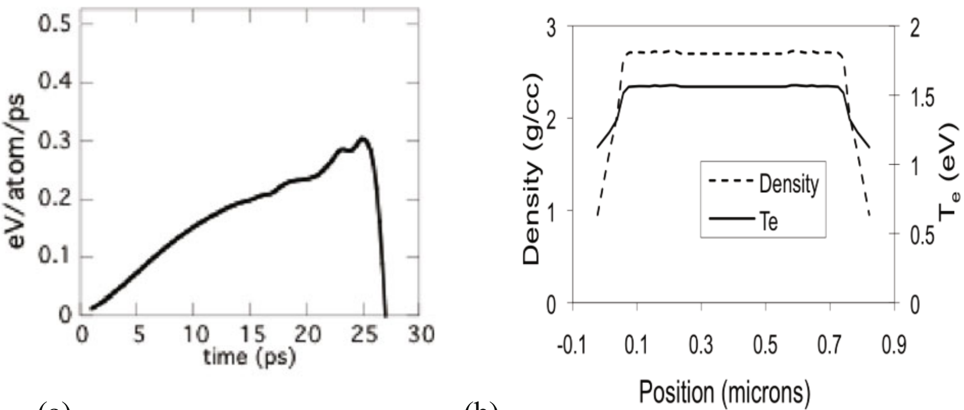

(a) (b)

Fig 8..(a) Temporal history of proton heating effect and (b) Resulting WDM conditions to be probed with an XRL beam of psec duration.

Summary

An experiment at the Vulcan laser has demonstrated that two-colour pumping can significantly boost the XRL output for targets with atomic number in the region of Z ~ 60 and this is probably due to an ability to access and heat plasma at a higher density with sufficiently small density gradients to avoid serious refraction problems. The TARANIS laser has been used to generate very bright beams of 18.9 nm and 13.9 nm XRLs and also proton beams with high fluence at up to ~12 MeV energy. We suggest an experiment to generate warm dense matter (WDM) conditions with protons to be diagnosed, with XRL photons as a means of validating equation of state (EOS) data.

Acknowledgements

The authors are grateful for financial support from the UK Engineering and Sciences Research Council under grants EP/C003586/1, EP/G007462/1 and EP/D06337X/1

References

1. Kawachi, T., et al.: 'Observation of strong soft-x-ray amplification at 8:8nm in the transient collisional-excitation scheme' *Phys. Rev. A.*, 69, 033805, 2004.
2. King, R. E., et al.: 'Saturated x-ray lasers at 196 and 73 a pumped by a picosecond traveling-wave excitation' *Phys. Rev. A.*, 64, 053810, 2001
3. Pert, G. J.: 'Optimizing the performance of nickel-like collisionally pumped x-ray lasers' *Phys. Rev. A.*, 73, 033809, 2006
4. Pert, G. J.: 'Optimizing the performance of nickel-like collisionally pumped x-ray lasers. ii. lasers for the wavelength range 50-100 Angstrom' *Phys. Rev. A.*, 75, 023808, 2007
5. Kuba, J., et al.: 'Two-color transient pumping in Ni-like silver at 13.9 and 16.1 nm' *Phys. Rev. A.*, 62, 043808, 2000
6. Lin, J. Y., et al.: 'Travelling wave chirped pulse amplified transient pumping for collisional excitation lasers' *Opt. Comm.*, 166, 211-218, 1999
7. Collier, J., et al.: 'The travelling wave focus on Vulcan' *Central Laser Facility Annual Report*, 1, 209-210, 1997
8. Nersisyan, G., et al.:'TARANIS: A pump source for X-ray lasers' *X-ray Lasers 2008 - Springer Proc. in Physics.* 130, 65-70, 2009
9. Dzelzainis, T., et al.: 'Ni-like X-ray lasing action pumped by the TARANIS laser system' *Proc. SPIE (Soft X-ray lasers and Applications VIII*, 7451, 745119, 2009
10. Dzelzainis, T., et al.: 'The TARANIS laser: A multi-Terawatt system for laser-plasma investigations' *Laser and Particle Beams*, 28, 451-461, 2010

Source Development and Novel Applications of Laser-Driven Plasma X-ray Lasers in JAEA

T. Kawachi[1], N. Hasegawa[1], M. Nishikino[1], M. Ishino[1], T. Imazono[1], T. Ohba[1], T. Kaihori[1], M. Kishimoto[1], Y. Ochi[1], M. Tanaka[1], M. Koike[1], M. Kado[1], K. Namikawa[2], T. Suemoto[3], K. Terakawa[3], T. Tomita[4], M. Yamamoto[1,4], N. Sarukura[5], H. Nishimura[5], A. Y. Faenov[1], S. Bulanov[1] and H. Daido[6] and Y. Kato[7]

[1]Quantum Beam Science Directorate, Japan Atomic Energy Agency (JAEA)
[2]Department of Physics, Tokyo University of Science
[3]Institute of Solid State Physics (ISSP), University of Tokyo
[4]Faculty of Engineering, University of Tokushima
[5]Institute of Laser Engineering (ILE), Osaka University
[6]Applied Laser Technology Institute, Japan Atomic Energy Agency (JAEA)
[7]Graduate School for the Creation of New Photonics Industries (GPI)

Abstract. This paper gives an overview of recent progress in the study of laser-driven plasma x-ray lasers in Japan Atomic Energy Agency (JAEA). Fully spatial coherent plasma soft x-ray laser (SXRL) at 13.9 nm with 0.1 Hz repetition rate is now routinely used in the wide variety of the applications: The highlights of these applications are the study of fluctuation in the atomic structure of ferroelectric substances under the phase transition using double SXRL probe technique and the first observation of surface dynamics of laser ablation with 10 ps-time and 1 nm-depth resolution using a single-shot SXRL interferometer.

1 Introduction

Advent of transient collisional excitation (TCE) scheme makes it possible for us to realize small size coherent soft x-ray lasers (SXRLs) [1-3]. In Japan Atomic Energy Agency (JAEA), we have firstly demonstrated fully spatial coherent x-ray laser beam at the wavelength of 13.9 nm by the method of double targets, in which the first gain medium works as the soft x-ray oscillator and the second gain medium works as the soft x-ray amplifier [4]. Successive optimization of the pumping condition such as the intensity of the pump, the temporal separation of the pre- and main-pulses and travelling wave realizes high quality and intense x-ray laser beam. The typical

J. Lee et al. (eds.), *X-Ray Lasers 2010,* Springer Proceedings in Physics 136,
DOI 10.1007/978-94-007-1186-0_2,

parameters of SXRL in JAEA are the beam divergence of better than 1 mrad, 1 μJ output energy and more than 10^9 photons in the coherent volume [5].

In a view point of the applications of the SXRLs, one of the most serious limitations so far was the repetition-rate. Typical shot interval of CPA Nd:glass driver was ~ 10 min, and this prohibited many potential users from conducting application experiments. The GRIP (grazing incidence pumping) scheme induced breakthrough in this problem: The 5-10 Hz spatially coherent SXRL with several tens nJ output energy has been obtained by the combination with higher-order harmonics as the x-ray seeder [6].

While this high average power SXRL is powerful tool for the soft x-ray imaging and nano-fabrication using multiple-shot exposure, there is also strong interest and requirement from material scientists for the probe beam to observe *non-periodic* or *non-repeatable* ultra-fast phenomena. For examples, nano-meter scale deformation of domain structure of substances under the phase transition is essentially *unrepeatable* phenomena; therefore single-shot observation is indispensable to observe the temporal or spatial correlation function of the generation and annihilation of the domains. Laser ablation is also *unrepeatable,* and observation of transient behaviour from solid phase to plasma phase is quite interesting in the view points of not only solid state physics and plasma physics but also the industrial applications such as laser processing and welding.

In order to improve the repetition-rate of SXRL, JAEA x-ray laser group has upgraded the pumping laser driver in 2008. The new driver system, TOPAZ, which is based on CPA Nd:glass laser. The highlight of TOPAZ is the zigzag slab-type amplifier chain, which enables us to operate this system with 0.1 Hz repetition-rate [7]. By use of TOPAZ laser, now the spatially coherent SXRL beam at 13.9 nm is routinely used for the application researches with adding minor revisions to improve the performance.

2 Application of SXRLs

The 13.9 nm laser in JAEA has been used for wide variety of application researches, such as material science [8,9], plasma physics, atom and molecular physics [10], soft x-ray imaging and laser processing [11] under the collaborations with universities and other institutes. For the next 5 years, FY2010-2014, one of the main objectives of soft x-ray laser research program in JAEA is development of the method to observe nano-scale dynamics of ultra-fast phenomena in substances, therefore we continue these collaborations to establish the optical pump & SXRL probe using x-ray speckle technique, x-ray interferometer and x-ray diffraction imaging. On the other hand, interaction of short-pulse SXRL with matter is quite interesting in terms of industrial application such as nano-scale laser fabrication and warm dense matter physics which is the intermediate region of material science and plasma physics. In the following, we show several results of SXRL applications for these topics.

2.1 Observation of temporal correlation of fluctuation dynamics of domain of $BaTiO_3$ under the phase transition condition

A couple of years ago, we have firstly observed pico-second snapshot of domain-structure of ferroelectric substrates, $BaTiO_3$, by use of the x-ray laser speckle technique [8], and the successive experiment revealed the existence of collective dipole moments (polarization clusters) under the phase transition condition of $BaTiO_3$ [9]. We extended this technique to *double* SXRL probes and tried to reveal the temporal correlation function of the polarization clusters by comparing two speckle signals temporally separated by τ.

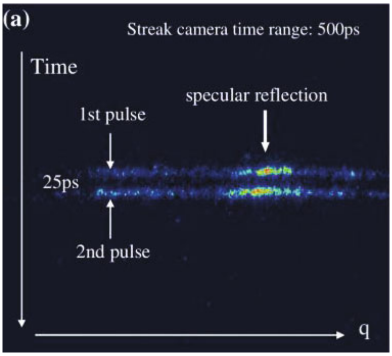

Fig.1. Soft x-ray speckle signal from double x-ray probes. From the comparison of these two speckles for various delay times, the temporal correlation of the domain fluctuation in $BaTiO_3$ is derived [12].

Temporal correlation of the two speckle signals is expressed by fourth order correlation of the scattered electric fields of SXRL pulses. The intensity correlation, $g^{(2)}$, is represented as follows.

$$g^{(2)} = \frac{\langle I(t)I(t+\tau)\rangle}{\langle I(t)\rangle_\tau^2} = 1+\beta \exp\left(-\frac{2\tau}{\tau_0}\right) \quad (1).$$

In Eq. (1), t and τ_0 is the time of the speckle measurement and the relaxation time of the polarization clusters. β is the square of the visibility defined by the first order correlation function of the incident electric fields of SXRL, *i.e.*, $E_0(t)$ and $E_0(t+\tau)$, where we assume that the delay is much larger than the relaxation time, *i.e.*, $\tau > \tau_0$.

In the experiment, the 13.9 nm laser was divided into two beams by Michelson-type double pulse generator based upon a free-stand Mo/Si multilayer beam splitter. With certain delay time, two x-ray laser pulses probed the surface of $BaTiO_3$, and we recorded two speckle signals in the different time by the x-ray streak camera. Figure 1 shows typical speckle signals obtained